Heat Transfer Research 45(5), 409–432 (2014)

EFFECT OF NANOFLUID VARIABLE PROPERTIES ON MIXED CONVECTION FLOW AND HEAT TRANSFER IN AN INCLINED TWO-SIDED LID-DRIVEN CAVITY WITH SINUSOIDAL HEATING ON SIDEWALLS

Mohammad Hemmat Esfe,[1] *Mohammad Akbari,*[1,*] *Davood Toghraie,*[2] *Arash Karimipour,*[1] *& Masoud Afrand*[1]

[1] *Department of Mechanical Engineering, Najafabad Branch, Islamic Azad University, Isfahan, Iran*

[2] *Department of Mechanical Engineering, Islamic Azad University, Khomeinishahr Branch, Isfahan, Iran*

[*]Address all correspondence to Mohammad Akbari
E-mail: makbari@pmc.iaun.ac.ir

In this study, mixed convection fluid flow and heat transfer in an inclined two-sided lid-driven cavity subjected to Al_2O_3–water nanofluid (with different particle diameters from 15 to 99 nm) has been investigated numerically. The geometry is a double lid-driven square cavity with sinusoidal temperature distribution on the left sidewall, while the right wall is kept at T_c. The top and bottom walls of the cavity, which move in opposite directions, are assumed to be insulated. The effects of inclination angle, Richardson number, nanoparticle volume fraction, temperature, and nanoparticle diameter based on recent variable property formulations are studied. The effects of an increase in Richardson number while the solid volume fraction is constant and effects of an increase in solid volume fraction when the Richardson number is kept constant are investigated. Also, the obtained results show that an increase in nanoparticle diameter influences the flow pattern and isotherm contours inside the cavity relatively when the Richardson number is kept constant and the diameter is varied from 15 to 99 nm. As the mean nanoparticle diameter increases, the corresponding flow velocity decreases, and hence the heat transfer enhancement is reduced. The results indicate that as Richardson number increases, the average Nusselt number rapidly increases for different values of d_p. Moreover, the results have clearly indicated that the addition of Al_2O_3 nanoparticles has produced a remarkable enhancement on heat transfer with respect to that of the pure fluid.

KEY WORDS: *nanofluid, variable properties, mixed convection, inclined cavity*

1. INTRODUCTION

Cooling systems are one of the most important concerns in the industries and everywhere that heat transfer is considered. In most cases, cooling optimization of existing heat transfer systems is done by increasing their heat transfer surfaces, which increas-

1064-2285/14/$35.00

NOMENCLATURE

c_p	specific heat, $J \cdot kg^{-1} \cdot K^{-1}$	*X, Y*	dimensionless Cartesian coordinates
Gr	Grashof number	**Greek Symbols**	
g	gravitational acceleration, $m \cdot s^{-2}$	α	thermal diffusivity, $m^2 \cdot s$
h	heat transfer coefficient, $W \cdot m^{-2} \cdot K^{-1}$	β	thermal expansion coefficient, K^{-1}
L	enclosure length, m	θ	dimensionless temperature
k	thermal conductivity, $W \cdot m^{-1} \cdot K^{-1}$	μ	dynamic viscosity, $kg \cdot m^{-1} \cdot s^{-1}$
Nu	Nusselt number	ν	kinematic viscosity, $m^2 \cdot s^{-1}$
p	pressure, $N \cdot m^{-2}$	ρ	density, $kg \cdot m^{-3}$
P	dimensionless pressure	φ	volume fraction of the nanoparticles
Pr	Prandtl number	γ	cavity inclination angle
U_0	lid velocity, $m \cdot s^{-1}$		
Re	Reynolds number		
Ri	Richardson number	**Subscripts**	
T	dimensional temperature, K	*c*	cold
u, v	dimensional velocity components in *x* and *y* directions, $m \cdot s^{-1}$	eff	effective
		f	fluid
U, V	dimensionless velocity components in *X* and *Y* directions	*h*	hot
		nf	nanofluid
x, y	dimensional Cartesian coordinates, m	*s*	solid particles
		w	wall

es the size of these devices, which is undesirable. Conversely, conventional fluids, such as water, ethylene glycol, and mineral oils, have a rather low thermal conductivity. Heat transfer in such devices can be enhanced by utilizing the nanofluid media. Nanofluids are engineered colloids made of a pure fluid and nanoparticles. Hence the heat transfer rate can be enhanced due to the higher thermal conductivity of these particles than the pure fluid (Choi et al., 2004). A comprehensive review of the nanofluid

heat behavior can be found in Godson et al. (2010), Sarkar (2011), and Mohammed et al. (2011).

Many investigators have studied various features of nanofluids (Godson et al., 2010). Some of them have been conducted about nanofluid in the enclosure. Wen and Ding (2005) studied a numerical model to survey heat transfer in a cavity filled with water–TiO_2 nanofluid heated from below. They used different models to evaluate the viscosity and effective thermal conductivity. Hwang et al. (2007) discussed the improvement of heat transfer in a nano-filled rectangular enclosure heated from bottom. Numerical simulation of natural convection in a cavity filled with water–copper nanofluid has been executed by Khanafer et al. (2003). Their results illustrated that the heat transfer rate increases as increasing the volume fraction of nanoparticles in a particular Grashof number.

Mixed convection, which combines both natural and forced convection, is a significant heat transfer mechanism that occurs in many applications. The most application of the mixed convection flow with lid-driven effect is to include the cooling of the electronic devices, lubrication technologies, drying technologies, food processing, chemical processing equipment, and so on. Owing to interaction of buoyancy and shear forces, mixed convection heat transfer is a complex phenomenon. Owing to the importance of this phenomenon, some studies have been applied on the mixed convection heat transfer in cavities filled with nanofluids.

For the first time, Tiwari and Das (2007) performed a numerical study on mixed convection heat transfer in a square cavity filled with the Cu–water nanofluid with differentially heated moving sidewalls and insulated top and bottom walls. Their investigation on the effects of the various parameters, such as volume fraction of the nanoparticles and Richardson number on the cavity heat transfer, proved that with increase in the volume fraction of the nanoparticles, for Richardson number equal to unity, the average Nusselt number increases.

In another study, a numerical simulation on mixed convection flow and heat transfer of Cu–water nanofluid in a lid-driven rectangular enclosure has been performed by Muthtamilselvan et al. (2010). The enclosure's sidewalls were insulated, while its horizontal walls were kept at constant temperatures, with the top wall moving at a constant velocity.

Guo and Sharif (2004) used the finite volume method and the SIMPLER algorithm to investigate the mixed convection in rectangular cavities at different aspect ratios with moving isothermal sidewalls and constant heat flux source on the bottom wall. They studied the impact of the heat source length, the Richardson number, and the aspect ratio of the cavity on the heat transfer. Their results showed that the average Nusselt number increased by moving the heat source toward the sidewalls.

The problem of the available classical models is their inability to evaluate the effective viscosity and thermal conductivity of the nanofluids (Morshed et al., 2008). Ho et al. (2008) distinguished four recent models for the effective dynamic viscosity

and thermal conductivity of an alumina–water nanofluid on the natural convection in a square cavity. They concluded that the model used for the viscosity and the thermal conductivity of the nanofluid is an important factor to predict that the heat transfer inside the enclosure could be either increased or decreased with respect to that of the base fluid.

The investigation of mixed convection flow and heat transfer in a cavity subjected to a Cu–water nanofluid has been executed by Talebi et al. (2010) using the finite volume method. The top and bottom walls of the cavity were adiabatic, and its vertical walls were differentially heated. They reported that for a specific Reynolds number, with an increase in the volume fraction of nanoparticles, heat transfer inside the cavity is enhanced.

Abu-Nada and Chamkha (2010) investigated the effects of variable properties on natural convection in cavities subjected to Al_2O_3–water and CuO–water nanofluids. Their results indicated that the average Nusselt number is more affected by viscosity models than by thermal conductivity models at high Rayleigh numbers.

In another study, a numerical investigation of mixed convective heat transfer inside a right triangular lid-driven cavity filled with a water–Al_2O_3 nanofluid with an insulated horizontal wall, hot inclined wall, and moving cold vertical wall was done by Ghasemi and Aminossadati (2010). In their work, the impacts of two different downward and upward movements of the cold vertical wall, Richardson number, and nanoparticles volume fraction have been considered. They concluded that for all values of Richardson number, the heat transfer rate for each direction of the sliding wall motion is enhanced by increasing the solid volume fraction.

Mahmoodi (in press) conducted a numerical simulation on mixed convection of Al_2O_3 water nanofluid in rectangular cavities with a hot moving bottom lid and cold right, left, and top walls. Also, the effect of nanofluid variable properties on mixed convection in a square cavity has been investigated by Mazrouei Sebdani et al. (2012)

Recently, a numerical study has been performed by Arefmanesh and Mahmoodi (2011) to investigate uncertainty effects of dynamic viscosity models for a Al_2O_3–water nanofluid on mixed convection. Their square enclosure consists of two cold walls (left and right), a cold horizontal top wall, and a moving hot bottom wall. They used two different viscosity models and studied the effects of the solid volume fraction and Richardson number on the fluid flow and heat transfer inside the enclosure. They found that for both of the viscosity models, with increasing volume fraction of the nanoparticles, the average Nusselt number of the hot wall also increases. Our studies are focused on the mixed convection in a square double lid-driven inclined cavity filled with a Al_2O_3–water nanofluid based on recent models.

The latest proposed models by Jang et al. (2007) and Abu-Nada et al. (2010) have been used to calculate the dynamic viscosity. Also, the model of Xu et al. (2006) is used to calculate the thermal conductivity of a nanofluid in the current study. These

models depend on parameters such as diameter of nanoparticles, diameter ratio, temperature, and volume fraction of nanoparticles.

The cavity has a nonuniform sinusoidal temperature profile on the left wall, and its right side wall is kept at constant cold temperature.

According to the best knowledge of the authors, no investigation has been done so far about the effects of variable properties on mixed convection in the double lid-driven cavity with a nonuniform temperature profile filled with nanofluid at different cavity inclination angles. The results of this study can be used in many industrial applications such as the lubrication industry, float glass production technology, and food processing.

In this article, the influences of parameters such as Reynolds number, cavity inclination angle, Richardson number, temperature, volume fraction of nanoparticles, and nanoparticle diameter on the hydrodynamics and thermal characteristics are discussed.

2. MATHEMATICAL MODELING

Figure 1 shows a square double lid-driven cavity considered for the present study. The height and the width of the cavity are denoted by L. The length of the cavity perpendicular to its plane is assumed to be long enough, hence the problem is considered two-dimensional.

The cavity is heated from sinusoidal temperature distribution, which exists on the left wall, and is cooled from the right wall (T_c). The top-moving and bottom-moving

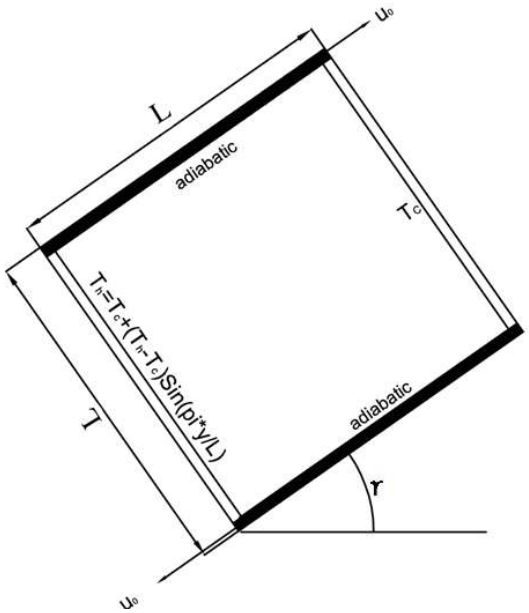

FIG. 1: Schematic of the current problem

TABLE 1: Thermophysical properties of water and nanoparticles at $T = 25°C$

Physical properties	Fluid phase (water)	Solid (Al_2O_3)
c_p, J/kg·k	4179	765
ρ, kg/m^3	997.1	3970
K, W·m^{-1}·K^{-1}	0.6	25
$\beta \times 10^{-5}$, 1/K	21.	0.85
$\mu \times 10^{-4}$, kg/ms	8.9	–
d_p, nm	–	47

walls move in their own plane at constant velocity U_0 and are supposed to be insulated. The cavity is filled with a suspension of Al_2O_3 nanoparticles with different particle diameters in water such that the nanoparticles and the base fluid are in thermal equilibrium and there is no slip between them.

The thermophysical properties of nanoparticles and the water as the base fluid at $T = 25°C$ are presented in Table 1.

The governing equations for a steady, two-dimensional laminar and incompressible flow are expressed as

$$\frac{\partial u}{\partial x} + \frac{\partial v}{\partial y} = 0 \ , \tag{1}$$

$$u \frac{\partial u}{\partial x} + v \frac{\partial u}{\partial y} = - \frac{1}{\rho_{nf}} \frac{\partial p}{\partial x} + \upsilon_{nf} \nabla^2 u \ , \tag{2}$$

$$u \frac{\partial v}{\partial x} + v \frac{\partial v}{\partial y} = - \frac{1}{\rho_{nf}} \frac{\partial p}{\partial y} + \upsilon_{nf} \nabla^2 v + \frac{(\rho\beta)_{nf}}{\rho_{nf}} g \Delta T \ , \tag{3}$$

$$u \frac{\partial T}{\partial x} + v \frac{\partial T}{\partial y} = \alpha_{nf} \nabla^2 T \ . \tag{4}$$

The dimensionless parameters may be presented as

$$X = \frac{x}{L}, \quad Y = \frac{y}{L}, \quad V = \frac{v}{u_0}, \quad U = \frac{u}{u_0},$$
$$\Delta T = T_h - T_c, \quad \theta = \frac{T - T_c}{\Delta T}, \quad P = \frac{p}{\rho_{nf} u_0^2}. \tag{5}$$

Hence

$$\mathrm{Re} = \frac{\rho_f u_0 L}{\mu_f}, \quad \mathrm{Ri} = \frac{Ra}{\mathrm{Pr} \cdot \mathrm{Re}^2}, \quad \mathrm{Ra} = \frac{g\beta_f \Delta T L^3}{\upsilon_f \alpha_f}, \quad \mathrm{Pr} = \frac{\upsilon_f}{\alpha_f}. \tag{6}$$

The dimensionless forms of the preceding governing equations (1)–(4) become

$$\frac{\partial U}{\partial X} + \frac{\partial V}{\partial Y} = 0, \tag{7}$$

$$U\frac{\partial U}{\partial X} + V\frac{\partial U}{\partial Y} = -\frac{\partial P}{\partial X} + \frac{\upsilon_{nf}}{\upsilon_f}\frac{1}{\mathrm{Re}} \cdot \nabla^2 U, \tag{8}$$

$$U\frac{\partial V}{\partial X} + V\frac{\partial V}{\partial Y} = -\frac{\partial P}{\partial Y} + \frac{\upsilon_{nf}}{\upsilon_f}\frac{1}{\mathrm{Re}} \cdot \nabla^2 V + \frac{Ri}{\mathrm{Pr}} \cdot \frac{\beta_{nf}}{\beta_f} \Delta\theta, \tag{9}$$

$$U\frac{\partial \theta}{\partial X} + V\frac{\partial \theta}{\partial Y} = \frac{\alpha_{nf}}{\alpha_f} \nabla^2 \theta. \tag{10}$$

2.1 Thermal Diffusivity and Effective Density

Thermal diffusivity and effective density of the nanofluid are, respectively,

$$\alpha_{nf} = \frac{k_{nf}}{(\rho c_p)_{nf}}, \tag{11}$$

$$\rho_{nf} = \varphi\rho_s + (1 - \varphi)\rho_f. \tag{12}$$

2.2 Heat Capacity and Thermal Expansion Coefficient

Heat capacity and thermal expansion coefficient of the nanofluid are therefore, respectively,

$$(\rho c_p)_{nf} = \varphi(\rho c_p)_s + (1 - \varphi)(\rho c_p)_f, \tag{13}$$

$$(\rho\beta)_{nf} = \varphi(\rho\beta)_s + (1 - \varphi)(\rho\beta)_f.$$

2.3 Viscosity

The effective viscosity of the nanofluid was calculated by

$$\mu_{eff} = \mu_f(1 + 2.5\varphi)\left[1 + \eta\left(\frac{d_p}{L}\right)^{-2\varepsilon} \varphi^{2/3}(\varepsilon + 1)\right]. \tag{14}$$

This well-validated model is presented by Jang et al. (2007) for a fluid containing a dilute suspension of small rigid spherical particles, and it accounts for the slip mechanism in nanofluids. The empirical constant ε and η are −0.25 and 280 for Al_2O_3, respectively.

It is worth mentioning that the viscosity of the base fluid (water) is considered to vary with temperature, and the flowing equation is used to evaluate the viscosity of water:

$$\mu_{H_2O} = (1.2723 \times {T_{rc}}^5 - 8.736 \times {T_{rc}}^4 + 33.708 \times {T_{rc}}^3 - 246.6 \times {T_{rc}}^2 + 518.78 \times T_{rc} + 1153.9) \times 10^6, \tag{15}$$

where $T_{rc} = \log (T - 273)$.

2.4 Dimensionless Stagnant Thermal Conductivity

The effective thermal conductivity of the nanoparticles in the liquid as stationary is calculated by the Hamilton and Crosser (1962) (H–C model):

$$\frac{k_{\text{stationary}}}{k_f} = \frac{k_s + 2k_f - 2\varphi(k_f - k_s)}{k_s + 2k_f + \varphi(k_f - k_s)} \tag{16}$$

2.5 Total Dimensionless Thermal Conductivity of Nanofluids

The following model was proposed by Xu et al. (2006):

$$\frac{k_{nf}}{k_f} = \frac{k_{\text{stationary}}}{k_f} + \frac{k_c}{k_f} = \frac{k_s + 2k_f - 2\varphi(k_f - k_s)}{k_s + 2k_f + \varphi(k_f - k_s)} + c\,\frac{\text{Nu}_p d_f \left(2 - D_f\right) D_f}{\text{Pr}\left(1 - D_f\right)^2} \frac{\left[\left(\frac{d_{\max}}{d_{\min}}\right)^{1-Df} - 1\right]^2}{\left(\frac{d\ \max}{d\ \min}\right)^{2-Df} - 1} \frac{1}{d_p}. \tag{17}$$

It has been chosen in this study to describe the thermal conductivity of nanofluids. The first term is the H–C model, and the second term is the thermal conductivity based on heat convection due to Brownian motion; c is an empirical constant, which is relevant to the thermal boundary layer and dependent on different fluids (e.g., c = 85 for the deionized water and c = 280 for ethylene glycol) but independent of the type of nanoparticles. Nu_p is the Nusselt number for liquid flowing around a spherical particle and is equal to 2 for a single particle in this work. The fluid molecular diameter $d_f = 4.5 \cdot 10^{-10}$ (m) for water in the present study. The Pr is the Prandtl number; φ and d_p are the nanoparticle volume fraction and mean nanoparticle diameter, respectively. The fractal dimension D_f is determined by

$$D_f = 2 - \frac{\ln \varphi}{\ln\left(\dfrac{d_{p,\min}}{d_{p,\max}}\right)}, \tag{18}$$

where $d_{p,\max}$ and $d_{p,\min}$ are the maximum and minimum diameters of nanoparticles, respectively. With the given/measured ratio of $d_{p,\min}/d_{p,\max}$, the minimum and maximum diameters of nanoparticles can be obtained with mean nanoparticle diameter d_p from the statistical property of fractal media. The ratio of minimum to maximum nanoparticles $d_{p,\min}/d_{p,\max}$ is R:

$$d_{p,\max} = d_p . \frac{D_f - 1}{D_f}\left(\frac{d_{p,\min}}{d_{p,\max}}\right)^{-1}, \tag{19}$$

$$d_{p,\min} = d_p . \frac{D_f - 1}{D_f} .$$

2.6 Nusselt Number

Nusselt number is

$$\mathrm{Nu} = \frac{hL}{k_f}, \tag{20}$$

where the heat transfer coefficient h is defined as

$$h = \frac{q_w}{T_h - T_c} \tag{21}$$

and the thermal conductivity may be expressed as

$$k_{nf} = \frac{-q_w}{\dfrac{\partial T}{\partial X}} . \tag{22}$$

By substituting Eqs. (18) and (19) into Eq. (17), the Nusselt number for the left hot wall can be written as

$$\mathrm{Nu} = -\left(\frac{k_{nf}}{k_f}\right)\left(\frac{\partial \theta}{\partial x}\right) . \tag{23}$$

The average Nusselt number calculated over the hot surface by Eq. (18) becomes

$$\mathrm{Nu}_m = \frac{1}{L}\int_0^L \mathrm{Nu}\, dY . \tag{24}$$

2.7 Boundary Conditions

The boundary conditions as set out earlier may be mathematically presented as

Left wall:

$$\begin{cases} U = V = 0 \\ \theta = \sin(\pi Y) \end{cases},$$

Right wall:

$$\begin{cases} U = V = 0 \\ \theta = 0 \end{cases},$$

Bottom wall:

$$\begin{cases} U = -1, V = 0 \\ \dfrac{\partial \theta}{\partial Y} = 0 \end{cases}, \tag{25}$$

Top wall:

$$\begin{cases} U = 1, V = 0 \\ \dfrac{\partial \theta}{\partial Y} = 0 \end{cases}.$$

3. NUMERICAL METHOD

Governing equations for continuity, momentum, and energy equations associated with the boundary conditions in this investigation were calculated numerically based on the finite volume method and associated staggered grid system, using FORTRAN computer code. The SIMPLE algorithm is used to solve the coupled system of governing equations. The convection term is approximated by a hybrid scheme that is conducive to a stable solution. In addition, a second-order central differencing scheme is utilized for the diffusion terms. The algebraic system resulting from numerical discretization was calculated utilizing TDMA applied in a line going through all volumes in the computational domain. The solution procedure is repeated until the following convergence criterion is satisfied:

$$error = \frac{\sum_{j=1}^{j=M} \sum_{i=1}^{i=N} \left| \lambda^{n+1} - \lambda^{n} \right|}{\sum_{j=1}^{j=M} \sum_{i=1}^{i=N} \left| \lambda^{n+1} \right|} < 10^{-7}. \tag{26}$$

Here M and N correspond to the number of grid points in the x and y directions, respectively, n is the number of the iteration, and λ denotes any scalar transport quantity. To verify grid independence, a numerical procedure was carried out for nine different mesh sizes, namely, 21 × 21, 31 × 31, 41 × 41, 51 × 51, 61 × 61, 71 × 71, 81 × 81, 91 × 91, and 101 × 101. Average Nu of the right hot wall is obtained for each grid size, as shown in Fig. 2.

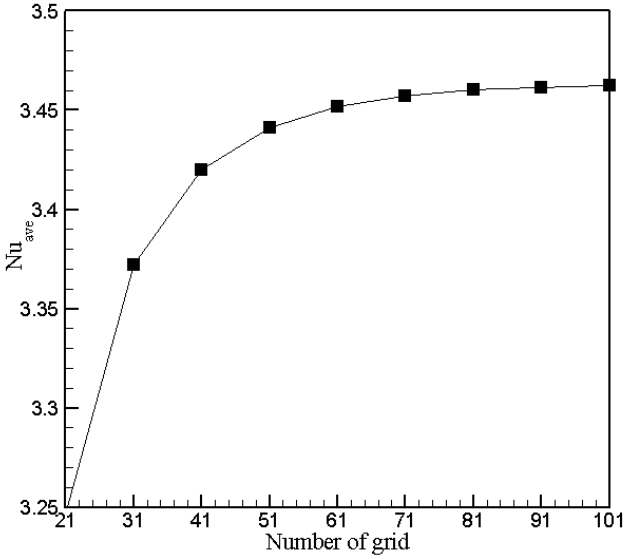

FIG. 2: Average Nusselt number for different uniform grids

As can be observed, an 81 × 81 uniform grid size yields the required accuracy and was hence applied for all simulation exercises in this work, as presented in the following section.

The proposed numerical scheme is validated by comparing the present code results for Gr = 10^5, d_p = 5 nm, φ = 0.05, and zero inclination angle for different values of Pr numbers against the numerical simulation published by Lin and Violi (2010) in Fig. 3. It is clear that the present code is in good agreement with another work reported in literature, as shown in Fig. 3.

Also, to ensure the accuracy and validity of this new model, we analyze a square cavity filled with base fluid with Pr = 0.7 and different Ra numbers. This system has been previously investigated by other researchers, such as Lin and Violi (2010), Tiwari and Das (2007), and Hadjisophocleous et al. (1998). Table 2 shows the comparison between the results obtained with the new model and the values presented in the literature. The quantitative comparisons for the average Nusselt numbers indicate an excellent agreement between them.

To check Xu's model, Fig. 4 indicates the characteristics of the effective thermal conductivity, which is a function of the practical parameters T, $R = d_{p,\min}/d_{p,\max}$, and d_p. As presented in Fig. 4a, R has relatively high impact for small average nanoparticle diameters. The temperature effect of nanofluids is illustrated in Fig. 4b. It is found that the existence of nanoparticles effects extensively on heat conductivity of the nanofluid at high temperatures. Thus, compared with the H–C model with the assumption of uniform nanoparticle size, Xu's model presents a better flexibility in predicting the heat transfer characteristics.

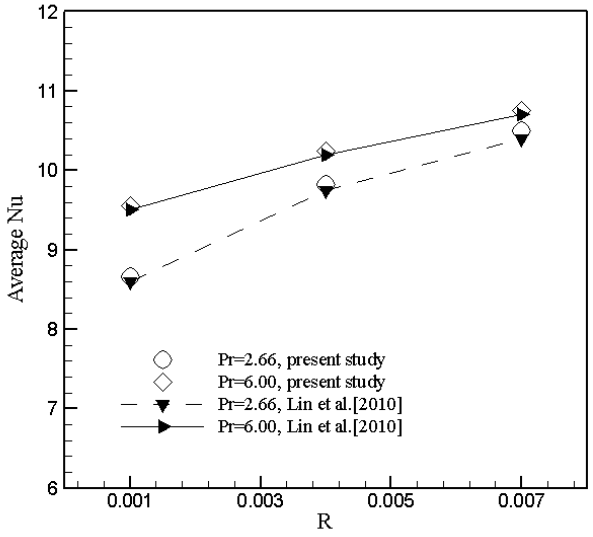

FIG. 3: Comparison of average Nusselt numbers between Lin and Violi (2010) and the present results for Gr = 10^5, d_p = 5 nm, and φ = 0.05 for different values of Pr numbers

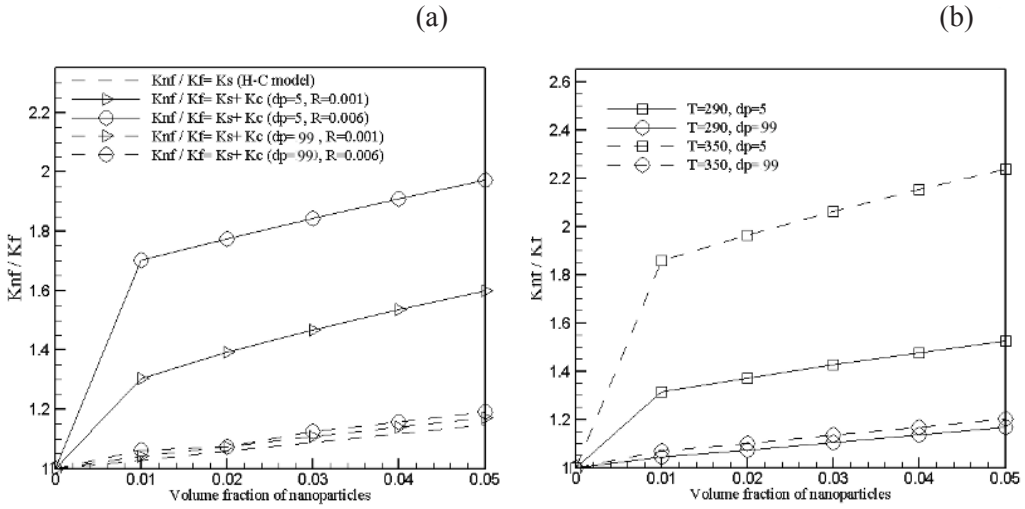

FIG. 4: Dimensionless effective thermal conductivity of Al_2O_3–water nanofluid versus concentration of nanoparticles with different mean nanoparticle diameters and fractal distributions: (a) T = 300 and (b) R = 0.004

TABLE 2: Code validation shows the comparison between the results in present study and other research

	Present study	Lin and Violi (2010)	Tiwari and Das (2007)	Hadjisophocleous et al. (1998)
(a) Ra = 10^3				
u_{max}	3.619	3.597	3.642	3.544
Y	0.811	0.819	0.804	0.814
v_{max}	3.697	3.690	3.7026	3.586
X	0.180	0.181	0.178	0.186
Nu_{ave}	1.114	1.118	1.0871	1.141
(b) Ra = 10^4				
u_{max}	16.052	16.158	16.1439	15.995
Y	0.817	0.819	0.822	0.814
v_{max}	19.528	19.648	19.665	18.894
X	0.110	0.112	0.110	0.103
Nu_{ave}	2.215	2.243	2.195	2.29
(c) Ra = 10^5				
u_{max}	36.812	36.732	34.30	37.144
Y	0.856	0.858	0.856	0.855
v_{max}	68.791	68.288	68.7646	68.91
X	0.062	0.063	0.05935	0.061
Nu_{ave}	4.517	4.511	4.450	4.964
(d) Ra = 10^6				
u_{max}	66.445	66.46987	65.5866	66.42
Y	0.873	0.86851	0.839	0.897
v_{max}	221.748	222.33950	219.7361	226.4
X	0.0398	0.03804	0.04237	0.0206
Nu_{ave}	8.795	8.757933	8.803	10.39

4. RESULTS AND DISCUSSION

In this article, a numerical analysis has been conducted to investigate the effects of inclination angles, Richardson numbers, nanoparticle volume fractions, temperature, and nanoparticle diameters on a nanofluid filling a two-dimensional inclined double lid-driven cavity with sinusoidal temperature distribution on the left wall.

The contours for different volume fraction of the nanoparticles, when d_p and inclination angle are kept fixed at 15 nm and 30°, respectively, and for different values

of Richardson number, are shown in Figs. 5–7. These figures demonstrate streamlines and isotherms for T = 300 K, R = 0.07 with different volume fractions of 0, 0.025, and 0.05, and Richardson numbers of 0.1, 1, and 10. For a constant Richardson

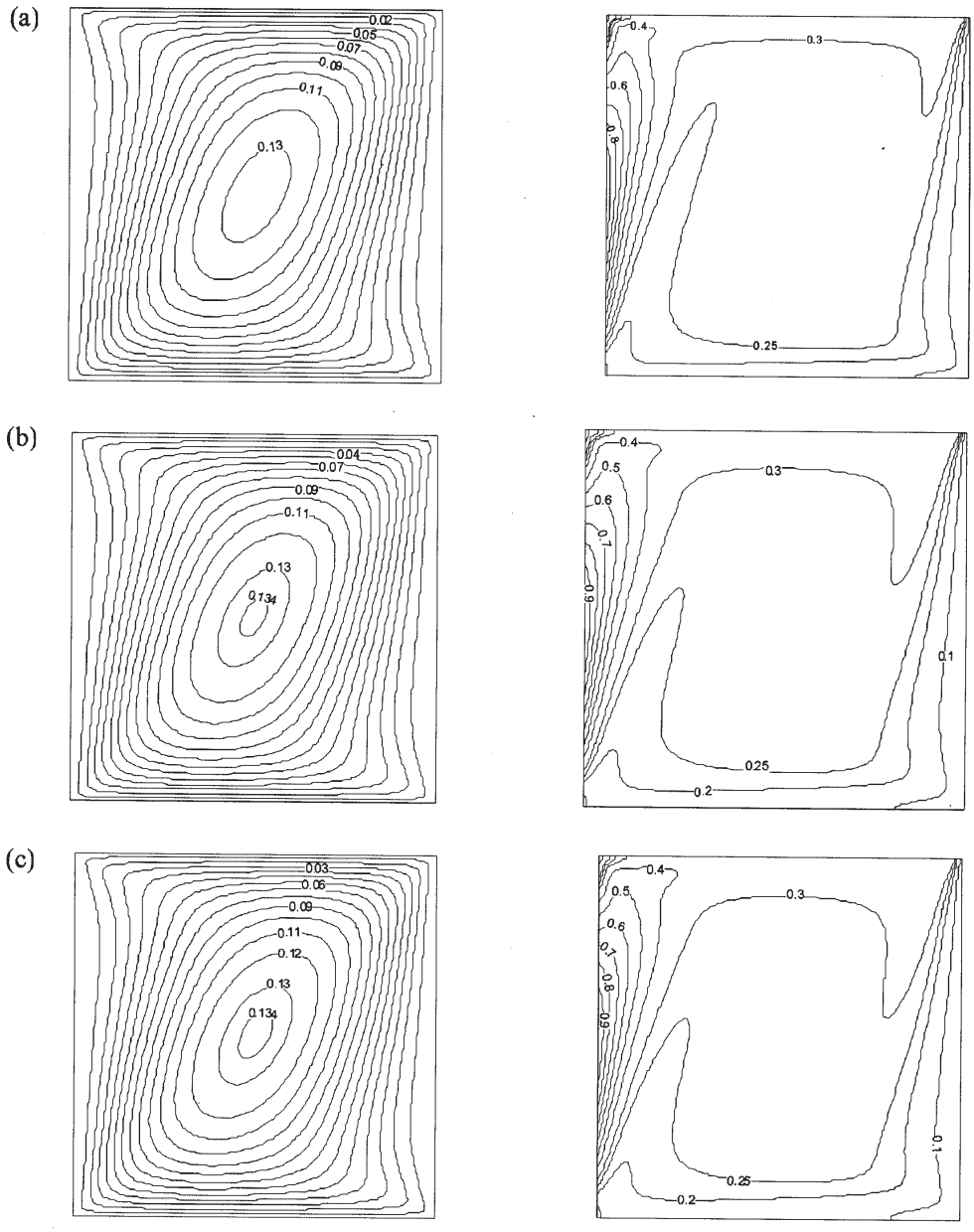

FIG. 5: Streamlines (on the left) and isotherms (on the right) for d_p = 15 nm, T = 300 K, R = 0.07, Ri = 0.1, and inclination angle of 30° with different volume fractions of (a) 0.0, (b) 0.025, and (c) 0.05

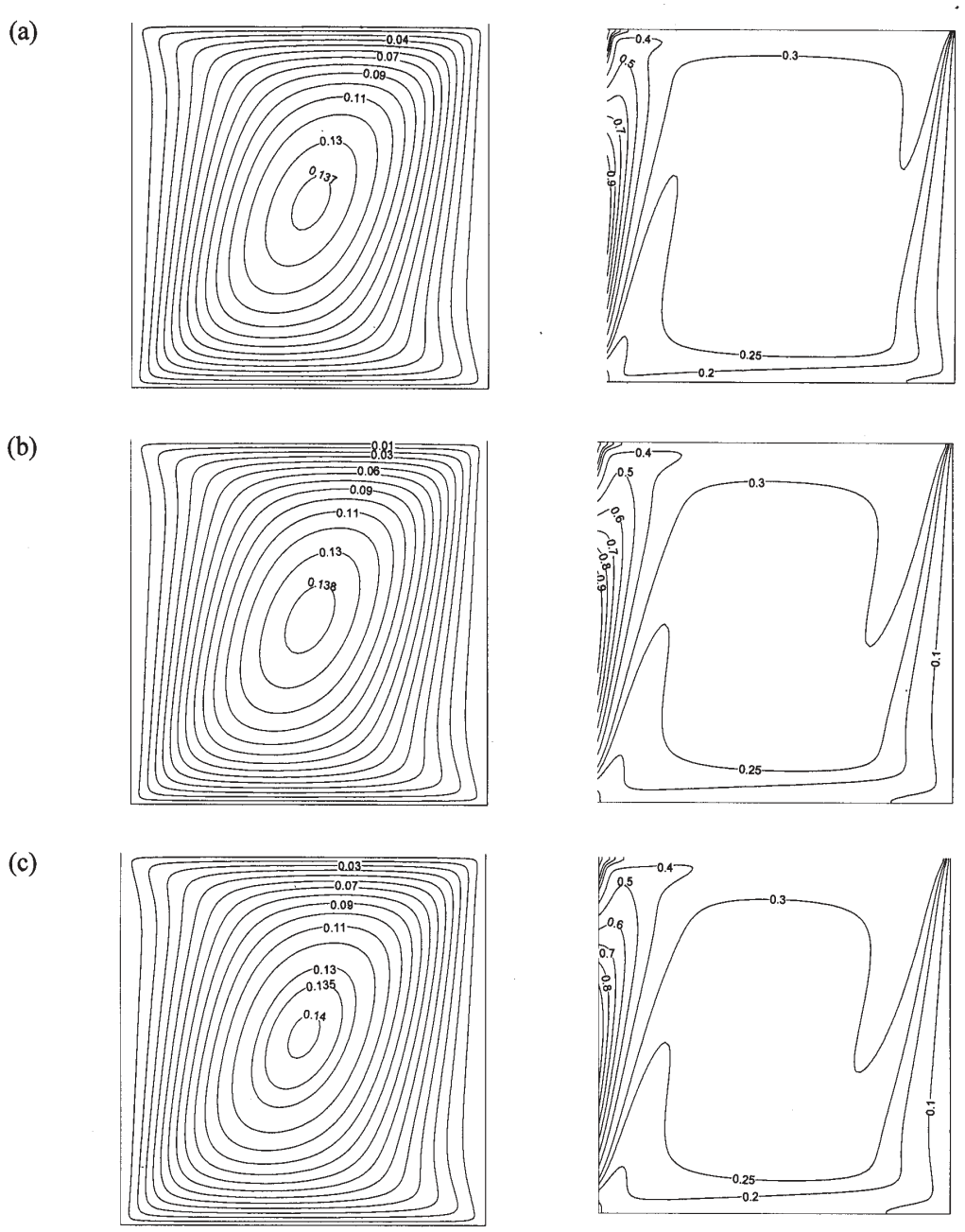

FIG. 6: Streamlines (on the left) and isotherms (on the right) for d_p = 15 nm, T = 300 K, R = 0.07, Ri = 1, and inclination angle of 30° with different volume fractions of (a) 0.0, (b) 0.025, and (c) 0.05

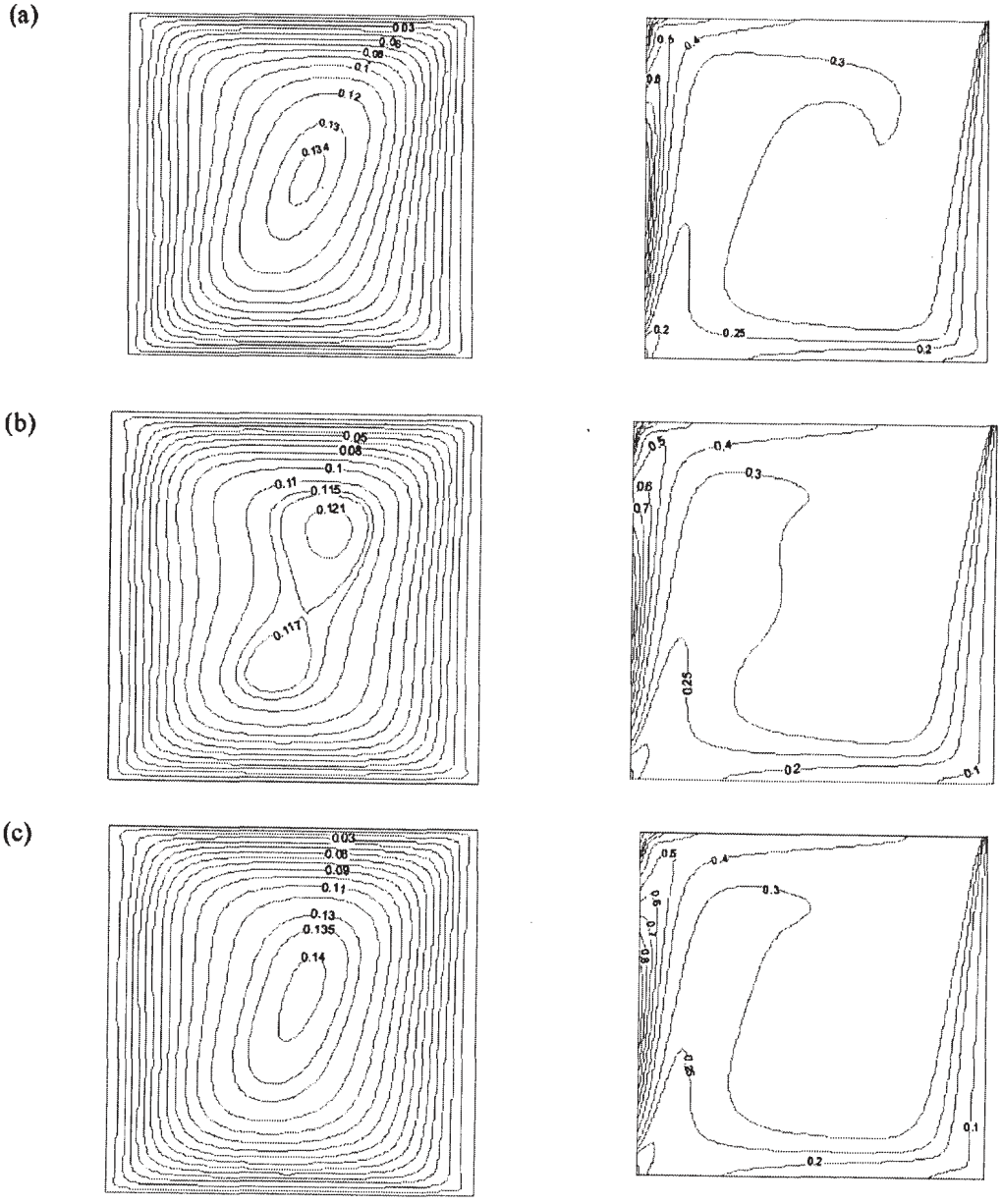

FIG. 7: Streamlines (on the left) and isotherms (on the right) for d_p = 15 nm, T = 300 K, R = 0.07, Ri = 10, and inclination angle of 30° with different volume fractions of (a) 0.0, (b) 0.025, and (c) 0.05

number, when the volume fraction of the nanoparticles increases, the convection heat transfer becomes more strongly limited. The contours describe the interaction between forced and natural convection. As can be found, an increase in solid concentration does not have a considerable effect on the thermal field.

As can be seen from the figures for all Richardson numbers and volume fractions of the nanoparticles, the nanofluid descends downward along the right wall, moves horizontally to the left corner of the cavity along the bottom wall, then moves upward and forms a counterrotating eddy inside the cavity. When Ri increases, the clockwise rotating vortex becomes larger due to greater absorption of energy from the wall with temperature distribution. Neither increase in Richardson number nor increase in nanoparticle volume fraction affects the flow pattern inside the cavity tremendously.

Effects of an increase in the nanoparticle concentration on flow and temperature fields are more distinguishable in Fig. 7. As can be found, the effect of nanofluid on the streamlines is more apparent for higher Ri. It is clearly seen that as the Richardson number increases to 10, the general manner of isotherms and streamlines is changed, so that in volume fraction of 0.025, the dominated central vortex is separated into two parts. Although an increase in Richardson number affects the contours in $\varphi = 0.025$, for other values of φ, no serious change is observed.

Figure 8 illustrates streamlines and isotherms for Ri = 10, $T = 300$ K, $R = 0.07$, and inclination angle of 60°. In this figure, the effect of diameter of nanoparticles on the mixed convection inside the cavity is investigated. The Richardson number is kept constant, and the diameter is varied from 15 to 99 nm. It is evident that an increase in nanoparticle diameter influences the flow pattern and isotherm contours inside the cavity relatively.

In this figure, conduction heat transfer is not strong, and the heat transfer occurs mainly through convection. As the diameter increases, the forced convection becomes stronger. As can be seen from the figure, with an increase in the diameter, the concentration of the isotherms in the sidewalls, especially the wall in temperature distribution, augments. It is an increase in thermal conductivity of the nanofluid that results in enhancement of diffusion of heat. Moreover, it can be seen than when the d_p increases, the core of the eddy becomes gradually smaller. With enhancement of the diameter, an augmentation in the value of dimensionless stream function is observed.

Figure 9 shows the effect of the nanoparticle diameter and inclination angle, respectively, on the heat transfer characteristics. This figure represents the variation of average Nu numbers with the inclination angles (0°, 30°, 60°, 90°) for Ri = 10, $T = 300$ K, $R = 0.07$, $\varphi = 0.05$, and different d_p of 15 nm, 40 nm, 70 nm, and 99 nm. It is obvious that average Nu decreases as angle of inclination increases. Inclination angle of the enclosure is proposed as a control parameter for fluid flow and heat transfer. It was found that lower heat transfer is formed for $\gamma = 90°$. Also, we see a significant decrease in average Nu number with increasing Al_2O_3 nanoparticle diameter.

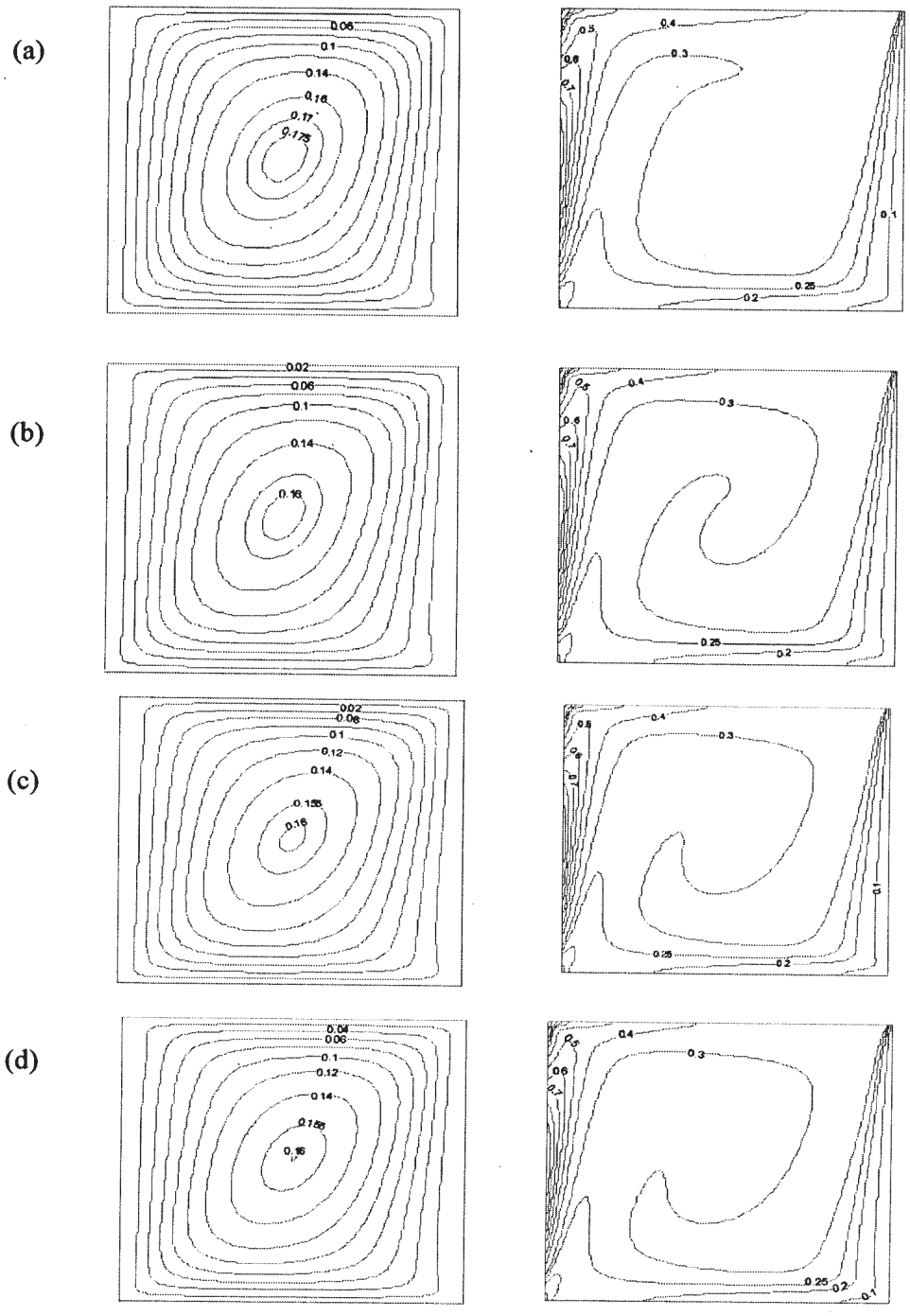

FIG. 8: Streamlines (on the left) and isotherms (on the right) for Ri = 10, T = 300 K, R = 0.07, and inclination angle of 60° with different values of d_p (a) 15 nm, (b) 40 nm, (c) 70 nm, and (d) 99 nm

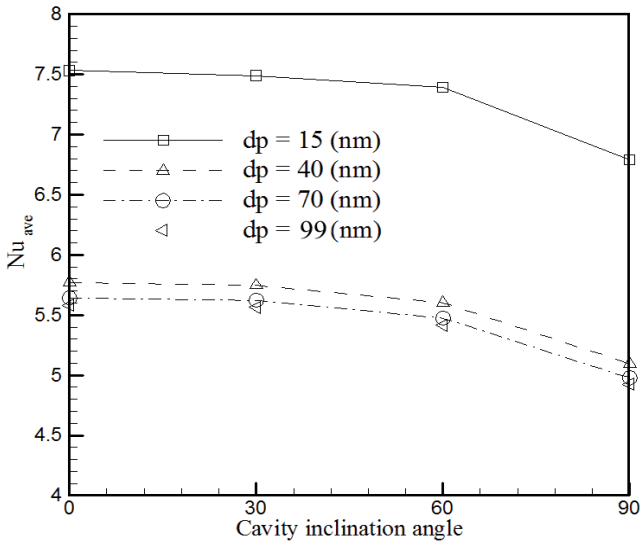

FIG. 9: Variation of average Nu numbers with the inclination angles for Ri = 10, T = 300 K, R = 0.07, φ = 0.05, and different d_p of (a) 15 nm, (b) 40 nm, (c) 70 nm, and (d) 99 nm

The influence of the nanoparticle volume fraction and inclination angle, respectively, on the average Nu number is reported by Fig. 10. This figure demonstrates the variation of average Nu numbers with the inclination angles (0°, 30°, 60°, 90°) for Ri = 10, T = 300 K, R = 0.07, d_p =15, and different φ of 0.0, 0.01, 0.02, 0.03, 0.04, and 0.05. It can be easily found from Fig. 10 that average Nu decreases as cavity inclination angle increases. The results have clearly indicated that the addition of Al_2O_3 nanoparticles has produced a remarkable enhancement on heat transfer with respect to that of the pure fluid.

We analyze the effect of Richardson number (from 0.1 to 10) and diameter of particles (from 15 to 99) on the heat transfer characteristics in Fig. 11. This figure illustrates the variation of average Nu numbers with the nanoparticle volume fractions for inclination angle of 0°, T = 300 K, R = 0.07, and different Ri and d_p. As d_p is increased from 15 to 99 nm, the average Nusselt number of nanofluids becomes considerably lower at each Richardson numbers of 0.1, 1, and 10. Also, the results indicate that as Ri increases, the average Nusselt number rapidly increases for different values of d_p.

To investigate the impact of the mean nanoparticle diameter on the velocity profiles, nanoparticle diameters are changed between 15 nm and 99 nm, while Ri, γ, and φ are fixed at 10, 60°, and 0.05, respectively. Figure 12 shows velocity profiles at the enclosure centerline for different values of d_p. As the mean nanoparticle diameter increases, the corresponding flow velocity decreases, and hence the heat transfer enhancement is reduced.

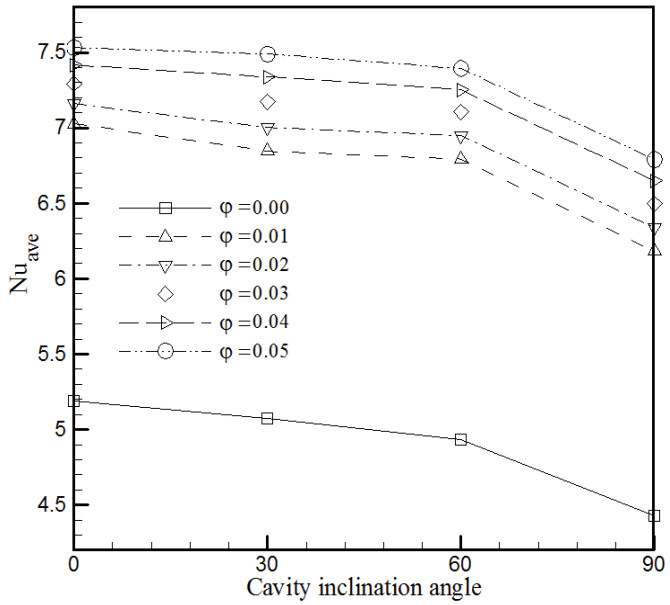

FIG. 10: Variation of average Nu numbers with the inclination angles for Ri = 10, T = 300 K, R = 0.07, d_p = 15, and different φ of 0.0, 0.01, 0.02, 0.03, 0.04, and 0.05

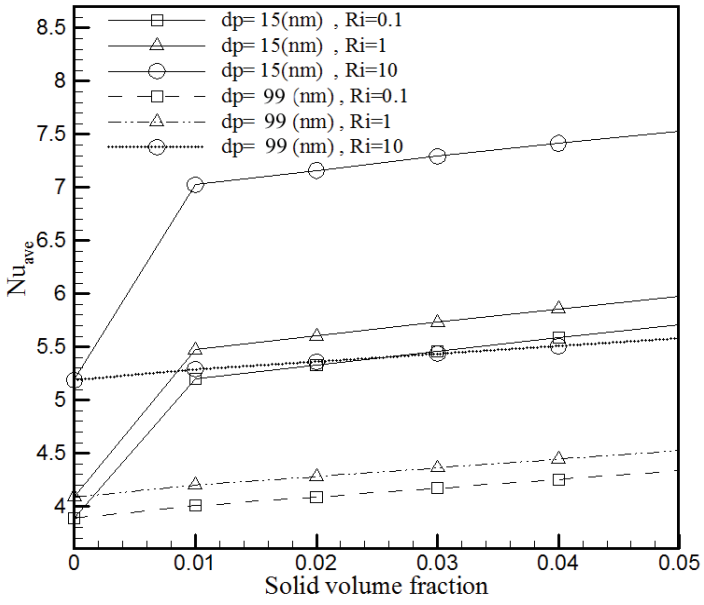

FIG: 11: Variation of average Nu numbers with the nanoparticle volume fractions for inclination angle of 0°, different d_p of 15 nm and 99 nm, and different Ri of 0.1, 1, and 10

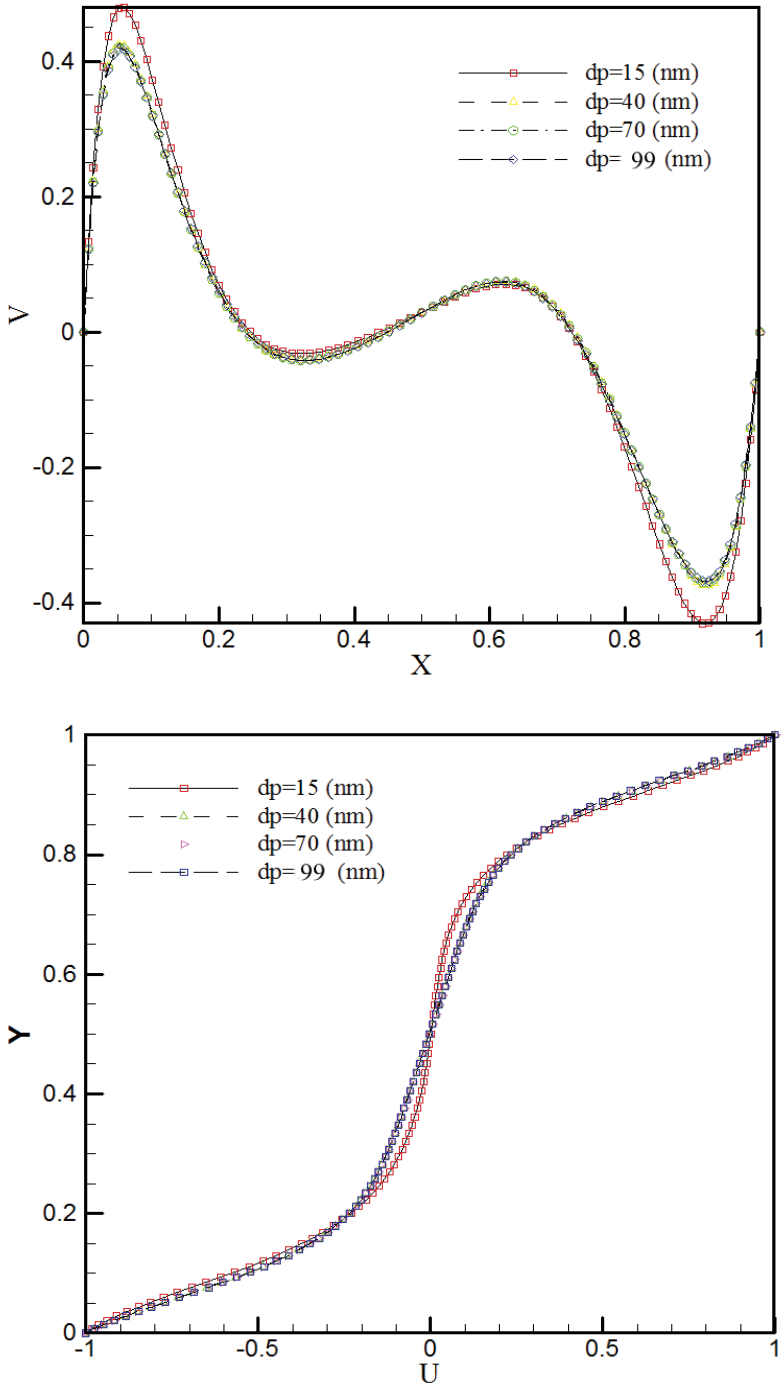

FIG: 12: Velocity profiles at enclosure centerline for different values of d_p with Ri = 10, inclination angle of 60°, and φ = 0.05

5. CONCLUSION

In this article, the influence of Al_2O_3–water nanofluid variable properties on mixed convection heat transfer in a two-dimensional inclined double lid-driven square cavity with sinusoidal temperature distribution on the left side wall was studied numerically. The developed numerical code was validated by comparing the obtained results with those available in the literature. We get the following conclusions from the obtained results:

1. When the nanoparticle volume fraction increases, while the Richardson number is kept constant, the convection heat transfer becomes more strongly limited. However, it is found that the increase in solid concentration does not have a considerable effect on the streamline contours at low Richardson numbers.

2. For all Richardson numbers and volume fractions of the nanoparticles, it is observed that the nanofluid descends downward along the right wall, moves horizontally to the left corner of the cavity along the bottom wall, then moves upward and forms a counterrotating eddy inside the cavity. When Ri increases, the clockwise rotating vortex becomes larger owing to greater absorption of energy from the wall with temperature distribution.

3. With increasing Richardson number, while the solid volume fraction is kept constant, the flow pattern inside the cavity tremendously is not affected. As can be found, the effects of an increase in the nanoparticle concentration on flow and temperature fields are more apparent at higher Richardson numbers. It is clearly seen that as the Richardson number increases to 10, the general manner of isotherms and streamlines is changed, so that in volume fraction of 0.025, the dominated central vortex is separated into two parts.

4. When the Richardson number is kept constant and the diameter is varied from 15 to 99 nm, it is evident that an increase in nanoparticle diameter influences the flow pattern and isotherm contours inside the cavity relatively. As the diameter increases, the forced convection becomes stronger, and concentration of the isotherms in the sidewalls augments.

5. It is obvious that average Nu decreases as angle of inclination increases.

6. The results have clearly indicated that the addition of Al_2O_3 nanoparticles has produced a remarkable enhancement on heat transfer with respect to that of the pure fluid.

7. As the mean nanoparticle diameter increases, the corresponding flow velocity decreases, and hence the heat transfer enhancement is reduced.

REFERENCES

Abu-Nada, E. and Chamkha, A. J., Mixed convection flow in a lid driven square enclosure filled with a nanofluid, *Eur. J. Mech. B Fluids*, vol. 29, pp. 472–482, 2010.

Abu-Nada, E., Masoud, Z., Oztop, H. F., and Compo, A., Effect of nanofluid variable properties on natural convection in enclosures, *Int. J. Thermal Sci*., vol. 49, pp. 479–491, 2010.

Arefmanesh, A. and Mahmoodi, M., Effects of uncertainties of viscosity models for Al_2O_3–water nanofluid on mixed convection numerical simulations, *Int. J. Thermal Sci*., vol. 50, pp. 1706–1719, 2011.

Choi, S. U. S., Zhang, Z. G., and Keblinski, P., Nanofluids, *Encyclopedia of Nanoscience and Nanotechnology*, vol. 6, pp. 757–773, 2004.

Ghasemi, B. and Aminossadati, S. M., Mixed convection in a lid-driven triangular enclosure filled with nanofluids, *Int. Commun. Heat Mass Transfer*, vol. 37, pp. 1142–1148, 2010.

Godson, L., Raja, B., Lal, D. M., and Wongwises, S., Enhancement of heat transfer using nanofluids — An overview, *Renew. Sust. Energy Rev.*, 14, pp. 629–641, 2010.

Guo, G. and Sharif, M. A. R., Mixed convection in rectangular cavities at various aspect ratios with moving isothermal sidewalls and constant heat flux source on the bottom wall, *Int. J. Thermal Sci*., vol. 43, pp. 465–475, 2004.

Hadjisophocleous, G. V., Sousa, A. C. M., and Venart, J. E. S., Predicting the transient natural convection in enclosures of arbitrary geometry using a nonorthogonal numerical model, *Numer. Heat Transfer A*, vol. 13, pp. 373–392, 1998.

Hamilton, R. L. and Crosser, O. K., Thermal conductivity of heterogeneous two component systems, *Indus. Eng. Chem. Fund.*, vol. 1 pp. 187–191, 1962.

Ho, C. J., Chen, M. W., and Li, Z. W., Numerical simulation of natural convection of nanofluid in a square enclosure: effects due to uncertainties of viscosity and thermal conductivity, *Int. J. Heat Mass Transfer*, vol. 51, pp. 4506–4516, 2008.

Hwang, K. S., Lee, J. H., and Jang, S. P., Buoyancy-driven heat transfer of water-based Al_2O_3 nanofluids in a rectangular, Cavity, *Int. J. Heat Mass Transfer,* vol. 50, pp. 4003–4010, 2007.

Jang, S. P., Lee, J. H., Hwang, K. S., and Choi, S. U. S., Particle concentration and tube size dependence of viscosities of Al_2O_3–water nanofluids flowing through micro- and minitubes, *Appl. Phys. Lett.*, vol. 91, pp. 24–31, 2007.

Khanafer, K., Vafai, K., and Lightstone, M., Buoyancy driven heat transfer enhancement in a two-dimensional enclosure utilizing nano fluids, *Int. J. Heat Mass Transfer*, vol. 46, pp. 3639–3653, 2003.

Lin, K. C. and Violi, A., Natural convection heat transfer of nanofluids in a vertical cavity: effects of non-uniform particle diameter and temperature on thermal conductivity, *Int. J. Heat Fluid Flow*, vol. 31, pp. 236–245, 2010.

Mahmoodi, M., Mixed Convection inside nanofluid filled rectangular enclosures with moving bottom wall, *Thermal Sci*., in press.

Mazrouei Sebdani, S., Mahmoodi, M., and Hashemi, S. M., Effect of nanofluid variable properties on mixed convection in a square cavity, *Int. J. Thermal Sci.*, vol. 52, pp. 112–126, 2012.

Mohammed, H. A., Bhaskaran, G., Shuaib, N. H., and Saidur, R., Heat transfer and fluid flow characteristics in microchannels heat exchanger using nanofluids: A review, *Renew. Sust. Energy Rev*., vol. 15, pp. 1502–1512, 2011.

Morshed, S. M. S., Leang, K. C., and Yang, C., Thermophysical and electrokinematic properties of nanofluids: A critical review, *Appl. Thermal Eng*., vol. 28, pp. 2109–2125, 2008.

Muthtamilselvan, M., Kandaswamy, P., and Lee, J., Heat transfer enhancement of copper–water nanofluids in a lid-driven enclosure, *Commun. Nonlinear Sci. Numer. Simul*., vol. 15, pp. 1501–1510, 2010.

Sarkar, J., A Critical review on convective heat transfer correlations of nanofluids, *Renew. Sust. Energy Rev*., vol. 15, pp. 3271–3277, 2011.

Talebi, F., Mahmoodi, A. H., and Shahi, M., Numerical study of mixed convection flows in a square lid-driven cavity utilizing nanofluid, *Int. Commun. Heat Mass Transfer*, vol. 37, pp. 79–90, 2010.

Tiwari, R. K. and Das, M. K., Heat transfer augmentation in a two-sided lid-driven differentially heated square cavity utilizing nanofluids, *Int. J. Heat Mass Transfer*, vol. 50, pp. 2002–2018, 2007.

Wen, D. and Ding, Y., Formulation of nanofluids for natural convective heat transfer applications, *Int. J. Heat Fluid Flow*, vol. 26, pp. 855–864, 2005.

Xu, J., Yu, B., Zou, M., and Xu, P., A new model for heat conduction of nanofluids based on fractal distributions of nanoparticles, *J. Phys. D*, vol. 39, pp. 4486–4490, 2006.